

# EFFECTS OF RADIOTHERAPY UPON BONE STRUCTURE-STRENGTH RELATIONSHIPS VARY WITH SEX AND FRACTIONATION OF DOSING

Maxwell Y. Sakyi, MS<sup>1</sup>; Benjamin J. Miller, MD, MS<sup>1</sup>; Mitchell C. Coleman, PhD<sup>1,3</sup>; Samuel N. Rodman, PhD<sup>3</sup>; Marc J. Brouillette, PhD<sup>1</sup>; Joshua E. Johnson, PhD<sup>1</sup>; Douglas C. Fredericks<sup>1</sup>; Jessica E. Goetz, PhD<sup>1,2</sup>

## ABSTRACT

**Background:** Radiotherapy for tumor treatment in or near bones often causes osteopenia and/or osteoporosis, and the resulting increased bone fragility can lead to pathologic fractures. Bone mineral density (BMD) is often used to screen for fracture risk, but no conclusive relationship has been established between BMD and the microstructural/biomechanical changes in irradiated bone. Understanding the effects of radiation dosing regimen on the bone structure-strength relationship would improve the ability to reduce fracture-related complications resulting from cancer treatment.

**Methods:** Thirty-two C57B6J mice aged 10 – 12 weeks old were randomized to single dose (1 x 25 Gy) and fractionated dose (5 x 5 Gy) irradiation groups. Right hindlimbs were irradiated while the contralateral hindlimbs served as the non-irradiated control. Twelve weeks after irradiation, BMD and bone microstructure were assessed with micro-computed tomography, and mechanical strength/stiffness was assessed with a torsion test. The effects of radiation dosing regimen on bone microstructure and strength were assessed using ANOVA, and bone strength-structure relationships were investigated through correlation analysis of microstructural and mechanical parameters.

**Results:** Fractionated irradiation induced significantly greater losses in BMD in the femur (23% - male mice,  $p=0.016$ ; 19% - female mice) and the tibia (18% - male mice; 6% - female mice) than the single-dose radiation. The associated reductions in trabecular bone volume (-38%) and trabecular

number (-34% to -42%), and the increase in trabecular separation (23% to 29%) were only significant in the male mice with fractionated dosing. There was a significant reduction in fracture torque in the femurs of male ( $p=0.021$ ) and female ( $p=0.0017$ ) mice within the fractionated radiation group, but not in the single dose radiation groups. There was moderate correlation between bone microstructure and mechanical strength in the single-dose radiation group ( $r = 0.54$  to  $0.73$ ), but no correlation in the fractionated dosing group ( $r=0.02$  to  $0.03$ ).

**Conclusion:** Our data indicate more detrimental changes in bone microstructure and mechanical parameters in the fractionated irradiation group compared to the single dose group. This may suggest the potential for protecting bone if a needed therapeutic radiation dose can be delivered in a single session rather than administered in fractions.

**Keywords:** micro-computed tomography, torsion, radiotherapy, bone morphometry, fractionation, osteopenia

## INTRODUCTION

Focal radiation therapy is a technique commonly employed to treat metastatic tumors to bone and soft tissue tumors adjacent to bone. Radiotherapy can be used with curative intent in definitive treatment, as a neoadjuvant to sterilize the peripheral margin or shrink a tumor before surgery, or as an adjuvant to limit local recurrence.<sup>1</sup> Radiotherapy is also used to relieve tumor-related pain that is not controlled with pain medications or pain that is localized to smaller regions, like in bone metastases. Metastases to bone are common in the spine, pelvis, humerus, and femur and cause significant morbidity due to the combination of pain and risk of pathological fracture through the metastatic lesion. Radiotherapy has been proven to significantly palliate painful bone metastases in 50-80% of patients with up to one-third of patients achieving complete pain relief at the treated site<sup>2</sup> and a 68% overall pain response rate.<sup>3</sup>

Unfortunately, confounding the positive therapeutic aspects of radiation therapy is the common development of osteopenia and/or osteoporosis, which can increase risk of fracture.<sup>4</sup> Bone fragility fractures are a common

<sup>1</sup>Department of Orthopedics and Rehabilitation, University of Iowa Hospitals and Clinics, Iowa City, Iowa, USA

<sup>2</sup>Department of Biomedical Engineering, University of Iowa, Iowa City, Iowa, USA

<sup>3</sup>Radiation Oncology Department, University of Iowa, Iowa City, Iowa, USA

Corresponding Author: Jessica E. Goetz, Ph.D., [jessica-goetz@uiowa.edu](mailto:jessica-goetz@uiowa.edu)

Disclosures: The authors report no potential conflicts of interest related to this study.

Sources of Funding: This work was supported by funding from the Iowa Sarcoma Multidisciplinary Oncology Group and NIAMS R01 AR070914.

late-onset complication that occur in bones within or underlying the radiation field.<sup>5</sup> Despite dose-limiting strategies developed to mitigate such side effects, the incidence of normal tissue injury and its subsequent complications tend to remain and even increase with time in cancer survivors. Post-radiotherapy complication rates are approximately 18%<sup>6</sup> overall but can range up to 45% for post-radiotherapy insufficiency fractures.<sup>7</sup>

Complication rates can be related to radiation dosage, which varies based on delivery method, treatment purpose, type of cancer, stage of cancer, spread, location, patient age, and patient health history.<sup>8</sup> The large radiation doses required for treatment are often delivered on a fractionated dosing schedule, which involves dividing the total desired dose into a series of smaller doses (fractions) delivered repeatedly over a specified time. For example, a typical fractionation dosage used for radiotherapy in curative treatment is 1.8 – 2 Gy per day over 6-8 weeks.<sup>9</sup> Fractionated radiotherapy exploits the differences in the repair capacities of tumor and normal tissues to maximize the therapeutic ratio, with the intention of reducing complications and increasing the rate of killing the tumor cells.<sup>9,10</sup> Fractionation also provides the opportunity to re-irradiate any tumor cells that were resistant during previous fractions. However, despite the benefits of fractionation, pathological fractures do still occur with a 5% incidence in fractionated radiotherapy-treated patients.<sup>11</sup> This is a clinical situation difficult to treat, often requiring multiple operative procedures and occasionally resulting in limb amputation. The persistence of pathological fracture in radiotherapy-treated patients has led to continuing investigation of the differential effects of fractionated and single dose treatment regimens on bone health.<sup>5,11-13</sup>

Bone strength is well known to be highly correlated to bone mineral density (BMD), and BMD is often used to screen for fracture risk.<sup>14</sup> However, BMD and several other bone parameters that correlate with bone strength for non-irradiated femurs have been found not to correlate with bone strength for irradiated femurs.<sup>5</sup> Furthermore, clinical studies of cancer survivors treated with radiotherapy have revealed no consistent relation between changes in bone mineral density and irradiation.<sup>15,16</sup> Such studies have shown significant increases<sup>16</sup>, decreases,<sup>17</sup> or no significant effect<sup>15,18</sup> of radiotherapy on BMD. Fractionation has also shown differential effects on bone. For example, Jia et al.<sup>6</sup> reported consistent 7.3% and 7.7% losses of BMD in mouse tibias and femurs, 14 days after a single 15 Gy radiation dose to the pelvic-abdominal cavity. However, in the fractionated group which was irradiated twice a day with 3 Gy for 7.5 consecutive days, there was a smaller 5.1% BMD loss in the tibia and a larger 13.8% BMD loss in the femur, 10 days after the

last radiation dose was administered. Many such studies are limited in their clinical applicability, as whole-body or torso radiation could introduce significant systemic effects that could influence bone density, and it is not reflective of the method of treating tumors in or near bones. Nevertheless, the inconsistencies in the effects of radiation dosing on BMD suggests a highly multifactorial response of irradiated bone that is likely due to wide variations in post-radiotherapy bone remodeling.<sup>5</sup>

A better understanding of the effect of specific aspects radiation therapy on the compositional, structural, and mechanical changes of bone may assist in developing strategies to mitigate the negative effects of radiation therapy in clinical settings.<sup>19</sup> The purpose of this study was to assess the effect of localized (non-systemic) single and fractionated radiation doses on bone strength, composition, and microstructure. We hypothesized that single high doses of radiation would result in greater loss of BMD, trabecular structure, and bone strength than a fractionated dosing regimen, but there would be little relationship between BMD and bone strength in either radiation dosing group.

## METHODS

Thirty-two C57B6J mice aged 10 – 12 weeks old were randomized to two different radiation study groups. Under IACUC-approved procedures, animals were sedated with an intraperitoneal injection of ketamine/xylazine and placed in a prone position inside protective lead boxes and the right hindlimbs were extended through a hole up to the hip and secured with adhesive (Figure 1). Depending on study group, the right hind limb

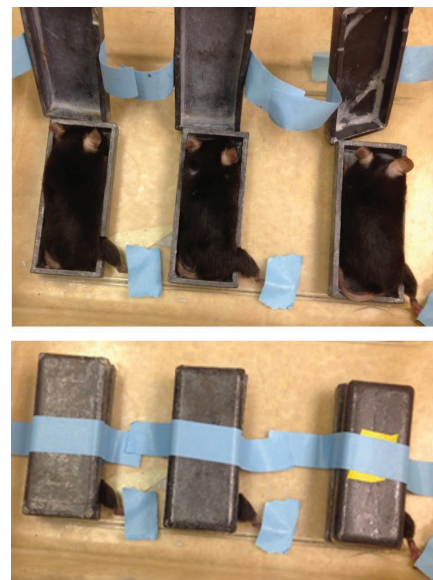


Figure 1. Protective lead shielding used to ensure only the right limb was irradiated during the study protocol.

was irradiated with one of two dosing regimens using a Pantak Therapax DXT 300 X-ray machine (200 kVp with added filtration of 0.35 mm copper and 1.5 mm aluminum). Group 1 (n=9 males; n=7 females) received a total radiation dose of 25 Gy (1×25 Gy) in a single session at a rate of 1.38 Gy/min (biological effective dose (BED) of 233.33 Gy). Group 2 (n=8 males; n=8 females) received a total 25 Gy in 5 Gy fractions delivered over a five-day period (5×5 Gy) (BED of 66.67 Gy). Animals recovered from sedation in isolation prior to returning to standard laboratory group housing conditions with up to 5 mice per enclosure. During the ensuing 12-week survival time, mice were housed on shavings and had free access to water and food. Animals were monitored daily by veterinary staff for overall health and by study team members for signs of radiation damage. A small number of animals that developed skin lesions at the radiation site were treated with topical ointment.

12 weeks post-irradiation, mice were euthanized, and both the irradiated and non-irradiated hind limbs were harvested for analysis. Superficial soft tissues were removed, leaving the periosteum intact. As freezing has been shown to not have any detrimental effect on the strength of the bone,<sup>20</sup> the femur and tibia were disarticulated, wrapped in saline-soaked gauze and frozen to -20°C in left/right pairs until subsequent micro-CT imaging and mechanical testing procedures.

### Micro-CT Acquisition & Analysis

Changes in bone morphology associated with radiation dosing regimen were evaluated using micro-computed tomography (micro-CT). Ex vivo scans of the dissected tibias and femurs were performed using the Skyscan 1176 scanner (Bruker, Kontich, Belgium) at 8.85 µm isotropic resolution (0.3° rotation steps over 180° rotation and frame averaging on). Approximately one third of the specimens, spanning both radiation groups, were scanned using a 0.5 mm Al filter (50 kV, 500 µA, 980 ms exposure time). However, this filter was unavailable when the second group of specimens were harvested, and a 1.0 mm Al filter (65 kV, 385 µA, 1037 ms exposure time) was used for the remaining specimens. For scanning, specimens were thawed to room temperature, aligned with the vertical axis of the scanner, and scanned in airtight containers while wrapped in saline-soaked gauze. Two 2 mm-diameter phantom rods with known mass concentrations of calcium hydroxyapatite (0.25 g/cm<sup>3</sup> and 0.75 g/cm<sup>3</sup>) were included in each scan for calibrating bone mineral density (BMD) calculations. Scans were reconstructed in the associated SkyScan NRecon software (v.1.6.1.1), using a modified Feldkamp cone-beam algorithm. Image compensation settings were as follows: generalized Hamming filter ( $\alpha=0.54$ ), 20%

beam hardening correction, 6% ring artifact correction, attenuation range 0 – 0.08.

DataViewer software (v 1.5.6.2) was used to reorient the resulting image volumes in the axial, coronal, and sagittal planes into a standard orientation for analysis. A metaphyseal volume of interest was extracted for both the femur and tibia by defining a location 0.05 mm<sup>5</sup> away from the distal and proximal growth plate, respectively, and extending 0.5 mm into the metaphysis (Figure 2). A diaphyseal volume of interest was defined for each bone beginning from a location 3 mm proximal or distal to the growth plate reference and extending 1 mm into the mid-diaphysis<sup>19</sup> (Figure 2).

An automated segmentation algorithm (CTAn software, v.1.20.3.0, SkyScan, Belgium) was customized to separate the trabecular and cortical bone regions in the extracted diaphyseal and metaphyseal volumes of interest for automated densitometric, structural, and morphometric parameter quantification. A density threshold of 0.502 g/cm<sup>3</sup> was chosen to isolate bone tissue. This



Figure 2. Volume of interest delineation from re-oriented micro-CT images. Proximal is up in both images. The reference slice in the femur is selected as the proximal-most edge of the growth plate and that of the tibia is selected as the distal-most edge of the growth plate. The proximal-most and distal-most slices were defined as those locations within the 3D volume and did not change on each image in the volume.



threshold was based on sensitivity to our image acquisition and reconstruction parameters and fell between the 0.35 g/cm<sup>3</sup><sup>19</sup> and 0.654 g/cm<sup>3</sup><sup>5</sup> range reported in the literature for micro-CT evaluation of irradiated mouse bones. Greyscale thresholds corresponding to the density threshold value were selected using the BMD-TMD to signal relationship provided by the inclusion of the calibration phantoms at the time of scan acquisition. For specimens in which both phantoms were not visible for the generation of this relationship, we used a density/intensity relationship that was the average of those generated for all other specimens that were scanned on that same day. Despite filtering, we observed that images acquired using the 1.0 mm Al filter contained more imaging noise, which interfered with the contrast along bone edges and therefore altered the automated region of interest selection. This was addressed by reconstructing the images with a lower maximum attenuation coefficient (0 – 0.06 range) which improved contrast enough for segmentation (delineation of the boundary region of contours within the volume of interest selection). These boundary contours were then applied to the original 0.08 maximum attenuation coefficient reconstructed images for morphometric quantification. Prior to morphometric evaluation, a square kernel, 1 voxel radius Gaussian filter was applied to reduce the inherent signal noise in the reconstructed micro-CT data.<sup>21</sup>

Densitometric, structural, and morphometric analyses were performed according to standard procedures.<sup>21</sup> Bone mineral density (BMD) was quantified for the metaphyseal regions and tissue mineral density (TMD) was quantified for the diaphyseal regions. Trabecular morphological measurements calculated for this work were tissue volume (TV), bone volume (BV), percent bone volume (BV/TV), trabecular thickness (Tb.Th)/separation (Tb.Sp)/number (Tb.N) and total porosity (Tb.Po). Cortical morphological measurements included tissue volume, bone volume, bone surface (BS) area, bone surface to volume ratio (BS/BV), bone surface density (BS/TV), cross-sectional thickness (Cs.Th), cross-sectional tissue area (Cs.T.Ar), and cross-sectional bone area (Cs.B.Ar).

### Mechanical Testing

Biomechanical torsional testing was performed using an electromechanical testing machine (MTS Insight, MN, USA). To interface with the testing device, a 3-mm self-drilling k-wire was threaded through the proximal and distal end of each bone, and the ends of the bone were potted in 6 mm × 6 mm square brass tubes using polymethyl methacrylate (PMMA). Bones that broke during handling were discarded (n= 2). For testing, the potted bones were thawed to room temperature and

affixed to the mechanical testing device by sliding the proximal end of the potted bone into a mating square holder that was attached to a 23.7 mm diameter cylindrical drum. A wire connected the drum to a 10 N load cell mounted on the vertical actuator, which when moved vertically caused the drum to rotate counterclockwise and applied torsion to the bone. The other end of the bone was held stationary with a leveling system comprised of a horizontally oriented metal bar clamp. The clamping mechanism height could be adjusted with washers to account for any uneven potting and ensure rotation occurred around the central axis of the bone (Figure 3). The tests were performed beginning from a slightly slack cable condition and ran in displacement control with a rate of 0.222 mm/s. This extension rate and drum diameter corresponded to a 0.21 degrees per mm rate of twist. Testing was manually stopped after an abrupt drop in the measured load-displacement curve. The load-displacement curves were used to calculate fracture torque, rotation at fracture, torsional stiffness, energy absorption capacity prior to failure, shear modulus, and maximum shear stress.

To calculate the torsional behavior of each specimen, the bones were approximated as a bar of homogenous material with a prismatic cross-section. With this assumption, the torsional angle of twist ( $\theta$  in radians) can be described by the equation:  $\theta = TL/GJ$  where T is the applied torsional moment, L is the gauge length, J is the polar moment of inertia of the cross-section, and G is the shear modulus of the bone. The denominator GJ represents the effective torsional rigidity of the specimen and is representative of the slope of the linear region of the

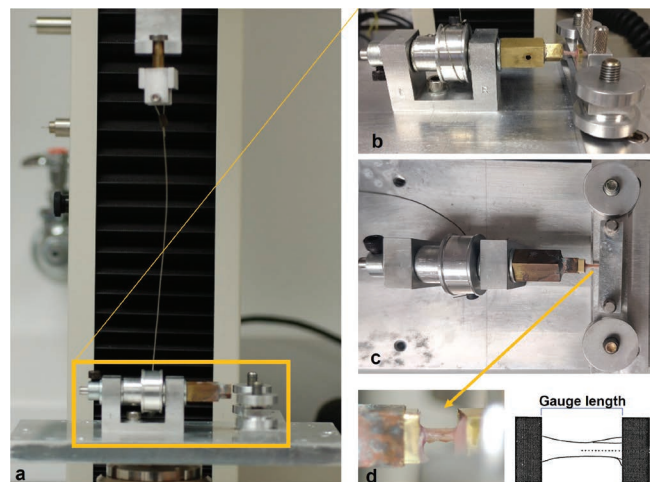


Figure 3a-d. Mechanical torsion testing setup. (3a) The cable connected to the vertical actuator to the rotating drum. (3b) Side view of a bone leveled horizontally and clamped for testing. (3c) Top-down view of a specimen positioned in the fixture for torsion testing. (3d) Zoomed-in side view of the bone positioned for testing (left) and schematic with the bone's central axis indicated (right).

torque-angle of twist curve. The polar moment of inertia,  $J$  was derived automatically by the CTAn software from a micro-CT image selected in the center of the diaphyseal region. Torsional stiffness was defined as the amount of torque per radian twist. The energy absorption capacity of the bones was defined as the area under the curve of the torque-angle of twist curve. Maximum shear stress,  $\tau$ , across the surface of the bones was calculated as  $\tau = Tr/J$ . The outer radius of the bone,  $r$ , was measured before torsional fracture tests using a digital caliper.

**Statistical Analysis**

Results are presented as means  $\pm$  standard deviations. Percentage changes are reported as the difference between the irradiated and non-irradiated bones of a given animal relative to the non-irradiated value. 2-way ANOVA was used to assess the significance of differences in the bone morphometric parameters and mechanical strength data between the single and fractionated radiation dosing groups as well as between both sexes using the Graph-Pad Prism software. Significance was assumed when  $p < 0.05$ . Pearson correlation was used to determine the relationships between microstructural parameters and mechanical strength parameters independently for the single-dose and the fractionated dosing groups.

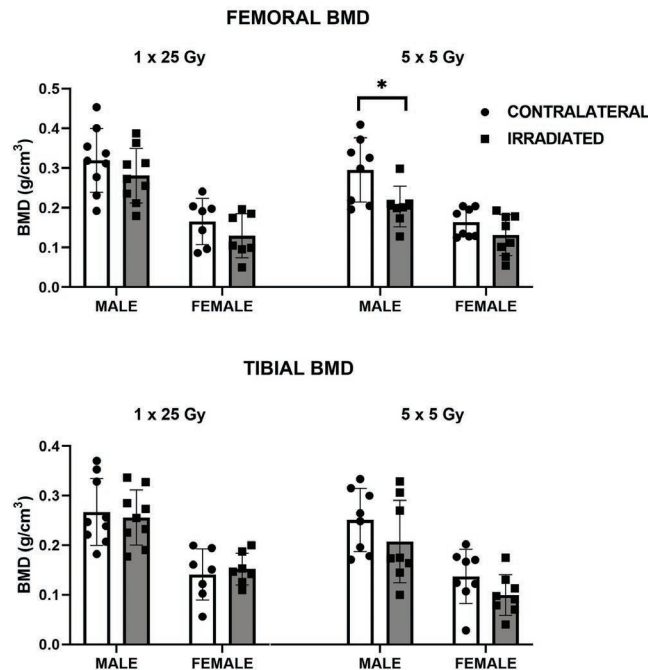


Figure 4. The differences in the effects of single dose (1 x 25 Gy) and fractionated dosing (5 x 5 Gy) on bone mineral density appeared to be sex related (\* $p=0.016$ ).

**RESULTS**

**Bone Density**

The BMD for the non-irradiated contralateral limbs in the female mice was significantly lower than that in the male mice for both the femur ( $p=0.0005$ ) and tibia ( $p=0.0004$ ). In both radiation dosing groups and in both male and female mice, the irradiated limb consistently had a lower bone mineral density (BMD) than the non-irradiated contralateral limb, however this trend only reached statistical significance ( $p=0.016$ ) in the femurs of the male mice in the fractionated dose group (Figure 4) with a 23% loss of BMD. Tissue mineral density (TMD) changes paralleled BMD changes, with a similar reduction of the TMD after radiation in all groups, but only reaching statistical significance ( $p=0.047$ ) in the femurs of the male fractionated group.

**Bone Microstructure**

In both the femur/tibia of male mice, there was a significant decrease in trabecular bone volume (-38% / -39%;  $p=0.0003$  /  $0.0014$ ), significant increase in trabecular separation (+23% / +29%;  $p=0.028$  /  $0.001$ ),

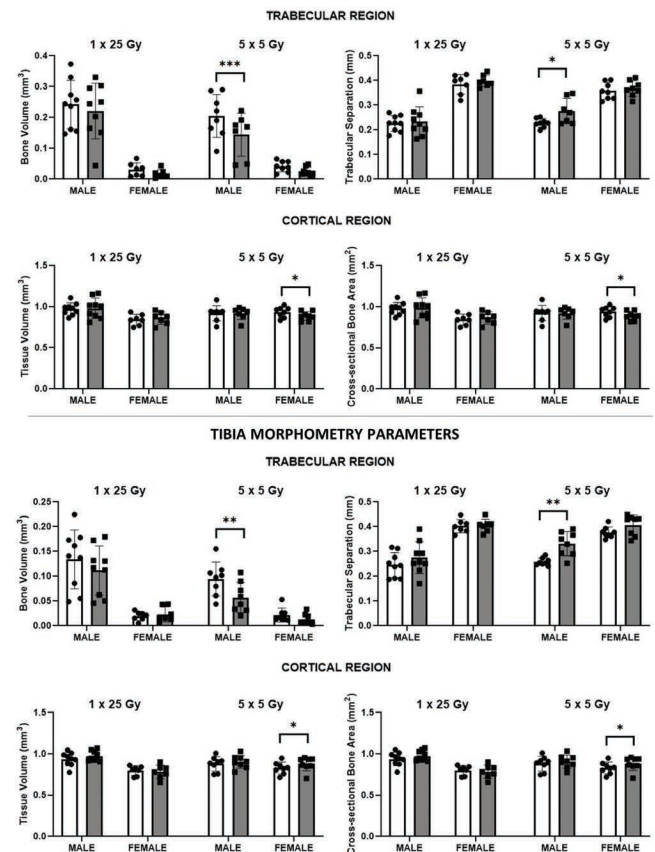


Figure 5. Femur Morphometry Parameters. Selected trabecular and cortical bone morphometric parameters demonstrated sex-related effects of single (1 x 25 Gy) and fractionated (5 x 5 Gy) dose on bone microstructure. \* $p < 0.05$ , \*\* $p < 0.01$ , \*\*\* $p < 0.001$ .

**Table 1. Statistical Significance of Radiation Effects on Bone Microstructure and Mechanical Parameters**

Bone Parameter		FEMUR				TIBIA			
		MALE		FEMALE		MALE		FEMALE	
		1×25Gy	5×5Gy	1×25Gy	5×5Gy	1×25Gy	5×5Gy	1×25Gy	5×5Gy
TRABECULAR REGION	BMD		↓*						
	TV								
	BV		↓***				↓**		
	BV/TV		↓**				↓**		
	Tb.Th								
	Tb.Sp		↑*				↑**		
	Tb.N		↓**				↓***		
	Tb.Po		↑**				↑**		
CORTICAL REGION MORPHOMETRY	TMD		↓*						
	TV				↓*				↑*
	BV				↓*				↑*
	BS/BV								↓**
	BS/TV								↓**
	Tb.Th			↑*					↑****
	Tb.N								↓****
	BS								
	Cs.T.Ar				↓*				↑*
	Cs.B.Ar				↓*				↑*
	Cs.Th			↑*					↑*
	MECHANICAL PARAMETERS	Tq		↓*		↓**			
EAC		↓**	↓***		↓****				
TR									
TS									
SM									↑*
MSS					↓*				↑**

For mechanical parameters: Tq= torque, EAC = energy absorption capacity, TR= torsional rigidity, TS = torsional stiffness, SM = shear modulus, MSS = maximum shear stress. Statistically significant change \*p<0.05, \*\*p<0.01, \*\*\*p<0.001, \*\*\*\*p<0.0001. ↑increase, ↓decrease.

and a significant decrease in trabecular number (-34% / -42%; p= 0.002 / 0.0001) in the irradiated limbs of the fractionated group compared to their non-irradiated contralateral limb (Figure 5). While similar trabecular microstructure changes were measured for the irradiated limbs of female mice in both radiation dosing regimens, as well as the male mice within the single radiation dose group, these changes were not statistically significant.

In the cortical regions, the most noticeable changes in bone morphometry were in the female mice that received fractionated radiation (Table 1). Interestingly, in

the cortical regions, significant decreases in quantities such as tissue volume associated with radiation paralleled those found in the trabecular bone, but only for the femur. In contrast, there were significant increases in tissue volume in the tibia of female mice with fractionated radiation (Figure 5).

**Mechanical Strength & Stiffness**

As would be expected from a torsion test, specimens mostly exhibited spiral fractures at failure (Figure 6). While there were some changes in bone mechanics

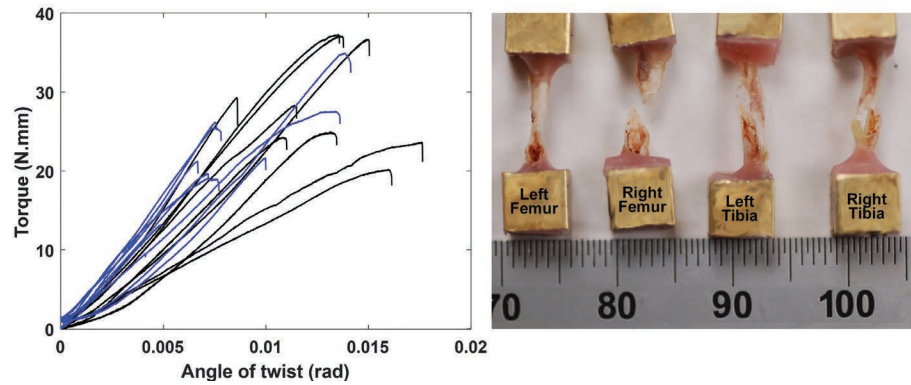


Figure 6. Torque-angle of twist curves measured for irradiated (blue) and contralateral (black) femurs from the single dose (1×25 Gy) irradiation group (left). This composite plot illustrates the consistency in the slopes of the linear regions of the curves, and the general stiffening that was associated with radiation. The wide range in torsional stiffness and failure torque of the non-irradiated group was decreased with radiation. Composites from tibia tests and tests of the fractionated dosing groups were similarly clustered. Typical spiral fracture patterns resulting from the torsion test are shown for the femur and for the tibia (right). The ruler is showing units of millimeters.

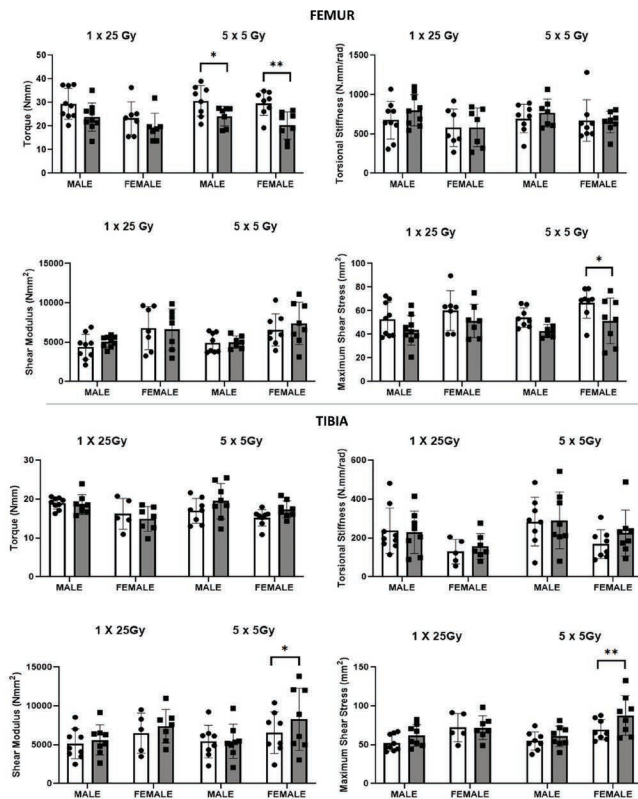


Figure 7. Selected mechanical parameters showed the effects of single (1 × 25 Gy) and fractionated (5 × 5 Gy) dose were sex-related and varied by bone. \*p<0.05, \*\*p<0.01.

among the males in the single radiation group, the vast majority of the significant differences in mechanical parameters were in the fractionated dosing group (Table 1). There was a significant reduction in the torque at fracture in the femurs of both male (p=0.021) and female (p=0.002) mice within the fractionated radiation group (Figure 7), however, no significant change in failure torque was measured for the tibia. Irradiated bones generally had increased torsional stiffness (were stiffer) as compared to non-irradiated bones, however, the differences were not statistically significant in either dosage groups or between the sexes (Table 1). There was a significant decrease (p=0.020) in maximum shear stress in the femur of the female mice for the fractionated group. Like what was found in the cortical morphometry metrics for these mice, the opposite trend was found in the irradiated tibia. Specifically, there was a significant increase (p=0.003) in the maximum shear stress of the tibia among the female mice within the fractionated dosing group.

### Bone Morphology-Strength Relationship

Overall, there were few strong relationships found between the BMD, morphological parameters, and mechanical strength of the bones. For the single dose radiation group, trabecular and cortical bone volumes of the femur were only modestly positively associated with torsional stiffness (r=0.57, 0.54). Cortical cross-sectional bone and tissue area were also moderately positively associated with torsional stiffness in the femur (r=0.54, 0.54). Trabecular thickness was negatively associated with maximum shear stress for both the femur (r=-0.61) and the tibia (r=-0.53). In contrast, in the fractionated



dosing group, even the modest associations between microstructural parameters and mechanical measures disappeared. The femurs in the fractionated group showed no association between the trabecular and cortical bone volumes with torsional stiffness ( $r=0.34$ ,  $0.27$ ), no association between the cortical cross-sectional bone and tissue area with torsional stiffness ( $r=0.27$ ,  $0.27$ ) and further, no association between trabecular thickness and maximum shear stress ( $r=-0.13$ ).

This trend was repeated for all the correlations that were explored. There was a good correlation of fracture torque with BMD ( $r=0.73$ ) in tibia of the single radiation group. However, for the fractionated group, there was no correlation ( $r=0.15$ ). Torque at fracture for the tibia within the single radiation dose group was moderately associated with bone volume ( $r=0.55$ ), trabecular separation ( $r=-0.51$ ) and total porosity ( $r=-0.53$ ). Again, the fractionated group showed no association between torque at fracture with bone volume ( $r=0.14$ ), trabecular separation ( $r=-0.02$ ) and total porosity ( $r=-0.10$ ).

## DISCUSSION

In this study, we confirmed local irradiation decreased trabecular bone mineral density and altered several components of bone microstructure. Loss of bone mineral density was pronounced in trabecular regions, with the most significant BMD decreases in the irradiated femurs of male mice. This trend did not reach statistical significance in the female mice, which could be attributed to the fact that the baseline trabecular BMD in the female mice was significantly lower than that of their male counterparts. The mechanical strength of the bones was also reduced by radiation, and the increase in torsional stiffness suggests embrittlement of the bone tissue. While the sex-related differences in irradiation effects were reversed in the cortical bone, with more detrimental effects found in the cortical regions in the female mice, the fractionated dosing consistently had a more pronounced effect than the single radiation dose.

Overall, our findings suggest that a single dose irradiation has less detrimental effects to the microstructure and mechanical strength of the bone than the fractionated dosage regimen. This may imply that reductions in the morbidity, i.e., fractures associated with radiation treatment, can be achieved with further refinement of patient radiotherapy fractionation schedules. A systematic review and meta-analysis of 25 randomized controlled trials of palliative radiotherapy,<sup>22</sup> compared single versus fractionated routines, finding overall response rates for intention-to-treat patients were 60% (from 2818 pooled randomizations) for single radiation dose treatment (8 Gy) and 61% (from 2799 pooled randomizations) for the fractionated treatment (30 Gy/10 fractions, 20 Gy/5 frac-

tions and 40 Gy/20 fractions). There was no significant difference in the overall response rate for pain between the dose fractionation schedules. Building on those findings, work by Bedard, et al.<sup>23</sup> reports equivalent pain relief outcomes between single and multiple fraction regimens and proposes adoption of single dose regimens for treatment of painful bone metastases. Single fraction treatment has also been proposed to optimize patient and caregiver convenience as well for cost-effectiveness (\$1099 vs \$2322).<sup>24</sup> As fractionation schedules become more varied for different malignancies, these results suggest that bone may be one tissue that will benefit from fewer fractions.

We elected to test our murine bones to failure using a torsion test rather than the often reported three-point bending and four-point bending tests. This approach was selected because the 15.3 to 16.7 mm lengths of our mouse bones were substantially shorter than the majority of reported rodent bone studies, which are performed in rat bones with lengths ranging from 34 to 46 mm.<sup>25</sup> Within those published studies, the fixed span and orientation of the bone within the testing setup influenced fracture pattern, stress distribution, and force-displacement relationships.<sup>25,26</sup> As the achievable fixed gauge length possible with the shorter mouse bones is significantly smaller than the 15 mm minimum used in rat studies,<sup>25</sup> a torsion test was utilized. The torque moment exerted in a torsional loading is the same in every section of the specimen along its entire length, and therefore, the result from the torsional test is less sensitive to experimental errors associated with directional alignment of the bones. Furthermore, torsion is a highly clinically relevant form of fracture failure.<sup>27</sup>

This study had several limitations that may have impacted the findings. First, the micro-CT images of the bones were scanned with two different scanner settings due to one of the filters being non-operational at the necessary post-euthanasia timepoint. While we were able to carefully adjust our analysis protocol to achieve equivalent segmentation edges and bone mineral density information, we cannot rule out systematically different bone morphometry data between batches that would slightly modify the relationship between morphometric measures and mechanical strength. Secondly, we did not perform limb loading analysis on these animals, which means that we cannot evaluate to what extent some of the osteoporosis identified was a result of changes in loading of the irradiated limb. However, during regular observation, no lameness was noted, and activity levels remained the same between groups. Another limitation of this work is the large difference in biological effective dose (BEDs) between groups. This was a result of choosing easily scalable fractions for delivery, rather than



hitting any specific therapeutic target. Nevertheless, the single dose BED (233.33 Gy) was higher than the fractionated dosing scheme (66.67 Gy) but resulted in fewer changes to the bone. Inclusion of a dosing scheme using the equivalent dose in 2 Gy fractions (EQD<sub>2</sub>) of the 5 x 5 Gy scheme (EQD<sub>2</sub>: 20 x 2 Gy) and direct comparison between the two could also shed light on the effect of increased fractionation on bone tissue. Finally, the very short gauge length available for testing after potting was further reduced for a few specimens which broke at the ends during k-wires drilling. Rather than discarding the specimen, when possible, the fractured end was disposed of, and the remainder potted, which in effect reduced the gauge length. Specimens that fractured during handling had to be discarded, effectively reducing our already relatively small sample size.

One other factor that cannot be ignored is the potential of a systemic reaction of the mice to the irradiation, which could cause changes to the bone in the non-irradiated contralateral limb. This is particularly important as results were assessed as left-to-right changes in microstructural and mechanical parameters. In a previous study,<sup>28</sup> it was found that in addition to the local effects at a localized site of irradiation (2 Gy), there was a 17% decrease in bone volume of the contralateral tibia relative to that of the tibia of non-irradiated control mice. These changes in the contralateral limb were accompanied by changes in associated microstructural parameters including increased trabecular separation and reduced trabecular thickness.<sup>28</sup> Similar work has found<sup>5</sup> significant loss of bending strength in the contralateral femurs of locally irradiated mice. This consideration of the systemic effects of irradiation is relevant as clinical studies have also reported systemic osteopenia in radiation-treated cancer patients.<sup>29,30</sup> This systemic effect would suggest that reporting our results relative to the non-irradiated contralateral would underestimate the impact of the radiation treatment on the irradiated limb. Nevertheless, changes in irradiated bone in this study parallel previously reported values in the range of 22% and 14% reductions in trabecular bone volume in the irradiated tibia and femur or decreases in trabecular number and increase in trabecular spacing/separation in the irradiated tibia (-16%/+20%) and femur (-13%/+16%).<sup>28</sup>

Recent advances to improve therapeutic ratio have introduced modified fractionation strategies including hyperfractionation and hypofractionation.<sup>10</sup> Hyperfractionation involves prolongation of treatment through delivery of radiation in small-dose fractions (2-3 times per day) with the advantage of avoiding acute reactions and allowing adequate reoxygenation in tumors. However, this approach does not spare late injury and may in fact allow the repopulation of tumor cells during treatment.<sup>31</sup>

In contrast hypofractionation involves the acceleration of treatment through delivery of smaller number of radiation fractions but with an increased dose per fraction. For example, breast cancers can be treated in three weeks (40 Gy in 15 fractions) as compared to the standard five weeks (50 Gy in 25 fractions).<sup>32</sup> In a systematic review,<sup>33</sup> it was shown that patients undergoing hypofractionation had a significantly reduced incidence of skin toxicity and no significant differences in the survival rates and tumor recurrences compared to standard fractionation. Our results also seem to support the concept of hypofractionation, as a single high dose of radiation resulted in less detrimental effects to the bone compared to a similar total dose delivered in smaller fractions. Optimal methods for delivering therapeutic radiation will continue to evolve, however, our findings would suggest that all other considerations being equal, the approach that utilizes the smallest number of fractions could be more protective of long-term bone strength.

#### ACKNOWLEDGEMENTS

This work was supported by funding from the Iowa Sarcoma Multidisciplinary Oncology Group and NIAMS R00 AR070914.

#### REFERENCES

1. **Hawley, L.** Principles of radiotherapy. *Br J Hosp Med (Lond)*, 2013. 74(11): p. C166-9.
2. **Lutz, S., L. Berk, E. Chang, et al.** Palliative radiotherapy for bone metastases: an ASTRO evidence-based guideline. *Int J Radiat Oncol Biol Phys*, 2011. 79(4): p. 965-76.
3. **Wong, E., P. Hoskin, G. Bedard, et al.** Re-irradiation for painful bone metastases - a systematic review. *Radiother Oncol*, 2014. 110(1): p. 61-70.
4. **Demirel, C., S. Kilciksiz, S. Gurgul, N. Erdal, and A. Yildiz.** N-acetylcysteine ameliorates gamma-radiation-induced deterioration of bone quality in the rat femur. *J Int Med Res*, 2011. 39(6): p. 2393-401.
5. **Oest, M.E., C.G. Policastro, K.A. Mann, N.D. Zimmerman, and T.A. Damron.** Longitudinal Effects of Single Hindlimb Radiation Therapy on Bone Strength and Morphology at Local and Contralateral Sites. *J Bone Miner Res*, 2018. 33(1): p. 99-112.
6. **Jia, D., D. Gaddy, L.J. Suva, and P.M. Corry.** Rapid loss of bone mass and strength in mice after abdominal irradiation. *Radiat Res*, 2011. 176(5): p. 624-35.
7. **Kwon, J.W., S.J. Huh, Y.C. Yoon, et al.** Pelvic bone complications after radiation therapy of uterine cervical cancer: evaluation with MRI. *AJR Am J Roentgenol*, 2008. 191(4): p. 987-94.

8. **Chauhan, S., S.A. Khan, and A. Prasad.** Irradiation-Induced Compositional Effects on Human Bone After Extracorporeal Therapy for Bone Sarcoma. *Calcif Tissue Int*, 2018. 103(2): p. 175-188.
9. **Allen, C., S. Her, and D.A. Jaffray.** Radiotherapy for Cancer: Present and Future. *Adv Drug Deliv Rev*, 2017. 109: p. 1-2.
10. **Mitchell, G.** The rationale for fractionation in radiotherapy. *Clin J Oncol Nurs*, 2013. 17(4): p. 412-7.
11. **Chow, E., Y.M. van der Linden, D. Roos, et al.** Single versus multiple fractions of repeat radiation for painful bone metastases: a randomised, controlled, non-inferiority trial. *Lancet Oncol*, 2014. 15(2): p. 164-71.
12. **Dewan, M.Z., A.E. Galloway, N. Kawashima, et al.** Fractionated but not single-dose radiotherapy induces an immune-mediated abscopal effect when combined with anti-CTLA-4 antibody. *Clin Cancer Res*, 2009. 15(17): p. 5379-88.
13. **Esenwein, S.A., S. Sell, G. Herr, et al.** Effects of single-dose versus fractionated irradiation on the suppression of heterotopic bone formation—an animal model-based follow-up study in rats. *Arch Orthop Trauma Surg*, 2000. 120(10): p. 575-81.
14. **Griffith, J.F. and H.K. Genant.** Bone mass and architecture determination: state of the art. *Best Pract Res Clin Endocrinol Metab*, 2008. 22(5): p. 737-64.
15. **Chen, H.H., B.F. Lee, H.R. Guo, W.R. Su, and N.T. Chiu.** Changes in bone mineral density of lumbar spine after pelvic radiotherapy. *Radiother Oncol*, 2002. 62(2): p. 239-42.
16. **Dhakal, S., J. Chen, S. McCance, et al.** Bone density changes after radiation for extremity sarcomas: exploring the etiology of pathologic fractures. *Int J Radiat Oncol Biol Phys*, 2011. 80(4): p. 1158-63.
17. **Okonogi, N., J. Saitoh, Y. Suzuki, et al.** Changes in bone mineral density in uterine cervical cancer patients after radiation therapy. *Int J Radiat Oncol Biol Phys*, 2013. 87(5): p. 968-74.
18. **Stutz, J.A., B.P. Barry, W. Maslanka, et al.** Bone density: is it affected by orchidectomy and radiotherapy given for stage I seminoma of the testis? *Clin Oncol (R Coll Radiol)*, 1998. 10(1): p. 44-9.
19. **Wernle, J.D., T.A. Damron, M.J. Allen, and K.A. Mann.** Local irradiation alters bone morphology and increases bone fragility in a mouse model. *J Biomech*, 2010. 43(14): p. 2738-46.
20. **Sammarco, G.J., A.H. Burstein, W.L. Davis, and V.H. Frankel.** The biomechanics of torsional fractures: the effect of loading on ultimate properties. *J Biomech*, 1971. 4(2): p. 113-7.
21. **Boussein, M.L., S.K. Boyd, B.A. Christiansen, et al.** Guidelines for assessment of bone microstructure in rodents using micro-computed tomography. *J Bone Miner Res*, 2010. 25(7): p. 1468-86.
22. **Chow, E., L. Zeng, N. Salvo, et al.** Update on the systematic review of palliative radiotherapy trials for bone metastases. *Clin Oncol (R Coll Radiol)*, 2012. 24(2): p. 112-24.
23. **Bedard, G., P. Hoskin, and E. Chow.** Overall response rates to radiation therapy for patients with painful uncomplicated bone metastases undergoing initial treatment and retreatment. *Radiother Oncol*, 2014. 112(1): p. 125-7.
24. **Konski, A. and M. Sowers.** Pelvic fractures following irradiation for endometrial carcinoma. *Int J Radiat Oncol Biol Phys*, 1996. 35(2): p. 361-7.
25. **Prodinger, P.M., D. Burklein, P. Foehr, et al.** Improving results in rat fracture models: enhancing the efficacy of biomechanical testing by a modification of the experimental setup. *BMC Musculoskelet Disord*, 2018. 19(1): p. 243.
26. **Osuna, L.G.G., C.J. Soares, A.B.F. Vilela, et al.** Influence of bone defect position and span in 3-point bending tests: experimental and finite element analysis. *Braz Oral Res*, 2020. 35: p. e001.
27. **Taylor, D., P. O'Reilly, L. Vallet, and T.C. Lee.** The fatigue strength of compact bone in torsion. *J Biomech*, 2003. 36(8): p. 1103-9.
28. **Wright, L.E., J.T. Buijs, H.S. Kim, et al.** Single-Limb Irradiation Induces Local and Systemic Bone Loss in a Murine Model. *J Bone Miner Res*, 2015. 30(7): p. 1268-79.
29. **Hopewell, J.W.** Radiation-therapy effects on bone density. *Med Pediatr Oncol*, 2003. 41(3): p. 208-11.
30. **Mitchell, M.J. and P.M. Logan.** Radiation-induced changes in bone. *Radiographics*, 1998. 18(5): p. 1125-36; quiz 1242-3.
31. **Salminen, E.K., K. Kiel, G.S. Ibbott, et al.** International Conference on Advances in Radiation Oncology (ICARO): outcomes of an IAEA meeting. *Radiat Oncol*, 2011. 6: p. 11.
32. **Haviland, J.S., J.R. Owen, J.A. Dewar, et al.** The UK Standardisation of Breast Radiotherapy (START) trials of radiotherapy hypofractionation for treatment of early breast cancer: 10-year follow-up results of two randomised controlled trials. *Lancet Oncol*, 2013. 14(11): p. 1086-1094.
33. **James M, H.B., Hider P, Jeffrey M.** Fraction size in radiation treatment for breast conservation in early breast cancer. (Protocol). 2002 4 June 2002 [cited 2002.